experimental data satisfactorily, with a different coefficient, as shown by the dashed line.

Given the above results, it is reasonable to use Eq. (10) to estimate the effects of sweep. Substituting Eq. (10) into Eq. (9) gives

$$\frac{\Gamma}{U_\infty} \sim \ell\,(\tan\epsilon)^{0.8} = \frac{\ell}{(\tan\Lambda)^{0.8}} \tag{11}$$

for fixed $\alpha$, demonstrating that the leading-edge vortex strength of delta wings with the same length decreases with increasing leading-edge sweep. Equation (11) can be expressed in terms of the planform area as

$$\frac{\Gamma}{U_\infty} \sim \frac{\sqrt{S_p}}{(\tan\Lambda)^{0.3}} \tag{12}$$

which shows that the previous statement is also true if $S_p$ is held constant. We also can write

$$\frac{\Gamma}{U_\infty} \sim \ell_{le}\frac{(\tan\Lambda)^{0.2}}{\sqrt{1+\tan^2\Lambda}} \tag{13}$$

where $\ell_{le}$ is the length of the wing leading edge. Using Eq. (13), it is easily shown that $\Gamma$ also decreases with increasing $\Lambda$ if $\ell_{le}$ is held constant ($\Lambda > 26.6$ deg). This is a useful result for variable sweep wings.

## Concluding Remarks

In this Note the difference between nonlinear lift and vortex lift has been distinguished. The nonlinear lift is the difference between the actual lift at a given $\alpha$ and that given by $K_p\alpha$. The vortex lift is the increment of lift above the zero leading-edge suction attached-flow lift and is due to the presence of the leading-edge vortex. Through the use of similarity and several experimental and computational results, it has been possible to show that the effect of increasing leading-edge sweep for slender delta wings is to decrease vortex lift and leading-edge vortex strength. These results are useful for the development of future design strategies for high angle-of-attack wing performance when it is desired to tailor the growth of the leading-edge vortices using sweep, camber, and leading-edge shape.

## Acknowledgments

The first author was supported in this work by the Transonic Aerodynamics Branch of NASA Langley Research Center under Contract NAS1-18000. The authors gratefully acknowledge many helpful discussions with E. C. Polhamus.

## References

[1]Polhamus, E. C., "A Concept of the Vortex Lift of Sharp-Edge Delta Wings Based on a Leading-Edge-Suction Analogy," NASA TN D-3767, Dec. 1966.

[2]Hemsch, M. J., "Similarity for High-Angle-of-Attack Subsonic/Transonic Slender-Body Aerodynamics," *Journal of Aircraft*, Vol. 26, No. 1, 1989, pp. 56–66.

[3]Sychev, V. V., "Three-Dimensional Hypersonic Gas Flow Past Slender Bodies at High Angles of Attack," *Journal of Applied Mathematics and Mechanics* (USSR), Vol. 24, Feb. 1960, pp. 296–306.

[4]Smith, J. H. B., "Calculations of the Flow over Thick, Conical, Slender Wings with Leading-Edge Separation," ARC R&M 3694, March 1971.

[5]Wentz, W. H., and McMahon, M. C., "Further Experimental Investigations of Delta and Double-Delta Wing Flow Fields at Low Speeds, NASA CR-714, Feb. 1967.

[6]Delery, J., Pagan, D., and Solignac, J. L., "On the Breakdown of the Vortex Induced by a Delta Wing," Colloquium on Vortex Control and Breakdown Behavior, Baden, Switzerland, ONERA TP 1987-105, April 6–7, 1987.

# Nonlinear Effects in the Two-Dimensional Adaptive-Wall Outer-Flow Problem

Edward T. Schairer*
*NASA Ames Research Center, Moffett Field, California 94035*

## Introduction

THE purpose of this Note is to examine the importance of nonlinear effects on the solution to the two-dimensional adaptive-wall outer-flow problem. The Note compares outer-flow solutions computed using the transonic small perturbation (TSP) equation with solutions based on the linear Prandtl-Glauert equation. Both methods are applied to simulated measurements of transonic flow past a two-dimensional airfoil in free air.

Wall settings for free-air flow are established in an adaptive-wall wind tunnel using flow measurements at or near the walls of the test section without any information about the model. This is possible since, in free air, redundant velocity distributions—for example, orthogonal components of velocity along a contour surrounding the model—are uniquely related. Thus, the walls can be adjusted until measured flow conditions satisfy these free-air relationships.[1]

The free-air relationships are derived by solving an outer-flow problem that is, in effect, a mathematical extension of the wind-tunnel flow from the contour to infinity. For a two-dimensional, rectangular contour extending upstream and downstream to infinity, the problem becomes that of solving for the flow in separate, infinite half-planes, one above and the other below the model, each subject to measured boundary conditions along the edge of the plane and free-air boundary conditions at infinity (vanishing perturbations).

Linear theory can be used to accurately represent most outer flows up to low transonic speeds, including many cases where flow near the model is quite nonlinear.[2,3] This is possible since perturbations, and thus nonlinear effects, are much smaller in the outer region than they are near the model. Linear solutions are convenient since they implicitly satisfy the free-air condition at infinity, can be derived analytically and expressed in closed form, and can be evaluated very quickly by a small computer.

It is inevitable that beyond some freestream Mach numbers, linear outer solutions will be inadequate. Unfortunately, there are no analytic solutions to even the simplest nonlinear equation, so approximate solutions can only be estimated, numerically or by other means. Since numerical solutions are computed in a finite domain, the free-air boundary condition at infinity cannot be applied directly. One approach to this problem is to transform the infinite physical domain into a finite computational domain.[4] Alternatively, if the numerical domain is simply a subset of the physical domain, either it must be large enough that use of zero perturbations provides a good approximation along its far-field boundaries or nonzero conditions must be estimated along less remote boundaries. Two two-dimensional experiments that used the large-domain approach have been reported.[4–6]

Received Jan. 14, 1989; revision received Oct. 30, 1989. 

*Aerospace Engineer, Fluid Dynamics Branch.

Restricting the size of the numerical domain has the obvious advantage of allowing nonlinear solutions to be computed in a shorter time using less computer memory. This is especially important in the adaptive-wall application where the solutions must be computed on line. Several methods for restricting the domain by estimating near-field boundary conditions have been published,[7-9] and their utility has been demonstrated in computations of transonic flow past two-dimensional airfoils. In the present Note, a similar method is applied to the adaptive-wall outer-flow problem.

The present work was done in preparation for adaptive-wall tests in the NASA Ames 2 × 2-ft transonic wind tunnel. The outer-flow solvers were designed to be applied to flow measurements at a set of discrete points and to be executed on line as part of the wall-setting algorithm. Thus, minimizing execution time was an important consideration. The linear solutions are based on well-known functional relationships; the nonlinear solutions are based on the TSP equation—the simplest equation that includes nonlinear terms—and were approximated in a rectangular subset of the physical domain by the method of finite differences. The size of the nonlinear domain was minimized by using linear theory to estimate nonzero free-air conditions along the far-field boundaries. The discussion will be limited to solutions for axial perturbation velocities $u$ computed from vertical-velocity boundary conditions $w$ along the edge of the upper half-plane.

## Linear Solutions

For flow that is governed by the linear Prandtl-Glauert equation, the free-air relationship between axial and vertical perturbation velocities along the edge of the infinite half-plane defined by $y \geq h$ is given by the Hilbert transformation[1]:

$$u(x,h) = \frac{1}{\beta\pi}\int_{-\infty}^{\infty} \frac{w(\xi,h)}{x-\xi}\,d\xi \tag{1}$$

where $x$ and $\xi$ are streamwise coordinates, $\beta = \sqrt{1-M^2}$, and $M$ is the freestream Mach number. For the present study, this equation was integrated numerically using data at a set of discrete points to represent the continuous upwash distribution in the integrand. The integral was truncated upstream and downstream of the airfoil at points corresponding to the ends of the 2 × 2-ft test section. For the cases described here, the upwashes at these end points were nearly zero, so the effect on the solution of truncating the integral was small.

## Nonlinear Solutions

The TSP equation was expressed in terms of the perturbation velocity potential $\phi$[10]:

$$(1-K^2)\frac{\partial^2\phi}{\partial x^2} + \frac{\partial^2\phi}{\partial y^2} = 0 \tag{2}$$

where

$$K^2 = M^2\left[1 + (1+\gamma)\frac{\partial\phi}{\partial x}\right]$$

The solution was approximated on a uniform, rectangular grid. All of the differential operators were replaced by second-order-accurate, central-difference operators at each grid point except that $\partial^2/\partial x^2$ was replaced by a second-order-accurate, upwind-difference operator at grid points where the flow was supersonic. No special shock-point operator was used, so the algorithm is nonconservative.

The numerical domain was a rectangle bounded on one side by the edge of the half-plane ($y = h$) and on the remaining three sides by far-field boundaries. Neumann boundary conditions, $(\partial\phi/\partial n)$, where $n$ is the inward normal to the boundary, were applied along all four boundaries. Along the edge of the half-plane, where $\partial\phi(\xi,h)/\partial n = w(\xi,h)$, the measured upwash could be applied directly. Had the far-field boundaries been sufficiently remote for the condition $\partial\phi/\partial n = 0$ to be appropriate, the computation time would have been excessive. Thus, nonzero free-air conditions were estimated along nearer far-field boundaries using the measured upwash and linear functional free-air relationships. For example, the free-air upwash boundary condition along the upper boundary $y = y_{FF}$ was computed using the one-component relationship[11]:

$$w(x,y_{FF}) = \frac{\beta|y_{FF}-h|}{\pi}\int_{-\infty}^{\infty} \frac{w(\xi,h)}{(x-\xi)^2 + \beta^2(y_{FF}-h)^2}\,d\xi \tag{3}$$

The difference equations were linearized locally and solved row by row, beginning with the row adjacent to the edge of the half-plane, with a successive line over-relaxation (SLOR) algorithm.

The present method is zonal in the sense that a nonlinear solution overlays the linear solution in the part of the outer flow nearest the model where perturbations are largest. The method forces only partial matching of the linear and nonlinear solutions at their interface: velocities normal to the far-field boundaries are forced to agree, whereas velocities parallel to the boundaries are not.

## Applications

The outer-flow solvers were applied to simulated data for an NACA 0012 airfoil in free air. Specifically, the computer program TSFOIL[12] was used to compute flow past the airfoil at zero incidence and Mach numbers 0.80, 0.85, and 0.90. Like the nonlinear outer-flow solvers, TSFOIL solves the TSP equation; unlike the outer-flow solver, however, the TSFOIL solutions were computed in the usual manner from local-surface slope boundary conditions applied along the airfoil chord and zero disturbance boundary conditions at the far-field boundaries. Axial and vertical velocities were extracted from the TSFOIL solutions at points in the flow where measure-

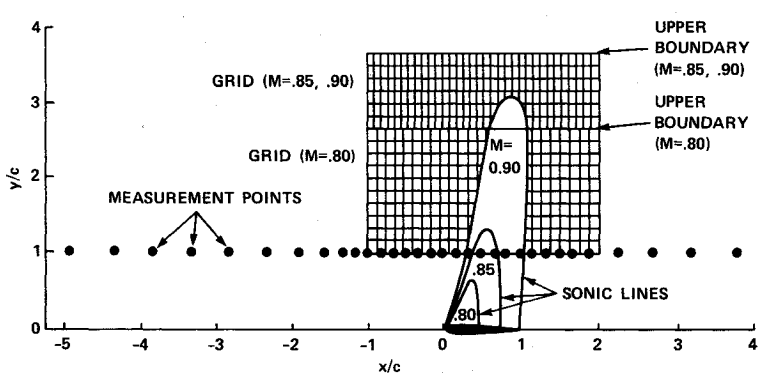


**Fig. 1 Measurement points, nonlinear domain and grid, and sonic lines for various freestream Mach numbers.**

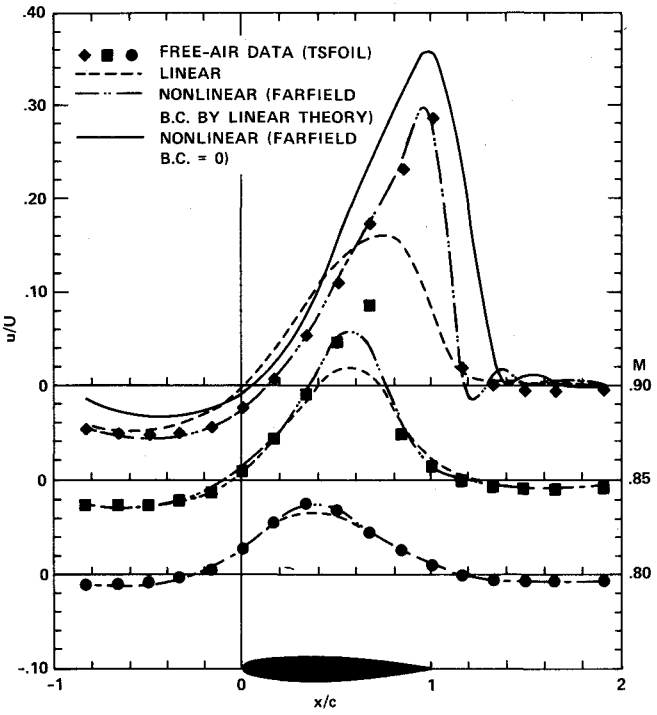


**Fig. 2 Comparison of linear and nonlinear solutions for $u$ along the lower boundary of the nonlinear domain.**

ments will be made in the 2 × 2-ft wind tunnel, i.e., along the boundary of the outer flow. Free-air axial velocities were estimated from the measured (TSFOIL) vertical velocities by solving the outer-flow problem. These were then compared to the free-air TSFOIL data.

The measurement points lay along the edge of the upper half-plane, an axial line one chord above the airfoil (Fig. 1). In the 2 × 2-ft wind tunnel, where laser velocimetry will be used to measure the velocities, the only constraint on the number of points will be the time allowed to make the measurements. The 32 points shown in Fig. 1 were chosen as a compromise between brevity in making the measurements and accuracy in representing the velocity distributions.

The domain for the TSP calculations extended from one chord upstream to two chords downstream of the airfoil leading edge. The height of the upper boundary, the number of streamwise mesh points, and the number of iterations of the algorithm differed for each case and depended on the extent of supercritical flow in the outer region. Each was chosen to be as small as possible without introducing significant errors in the solution (Fig. 1).

Figure 2 compares the linear and nonlinear outer-flow solutions for axial velocity along the measurement line with the free-air velocities computed using TSFOIL. The nonlinear solutions (dot-dash lines) are more accurate than the linear solutions (dotted lines) at all three Mach numbers. At $M = 0.80$, where the supersonic bubble does not penetrate into the outer flow (Fig. 1), the nonlinear effects are small and confined to the region immediately above the airfoil. At $M = 0.85$, the nonlinear effects are larger but still are very limited in extent. However, at $M = 0.90$, where there is substantial supercritical flow in the outer region, the linear and nonlinear solutions are quite different even upstream of the airfoil.

A Data General Eclipse S/200 minicomputer computed each linear solution in about 0.25 s and the nonlinear solutions for the cases $M = 0.80$, 0.85, and 0.90 in 16, 30, and 55 s, respectively (computation speed: $0.5 \times 10^6$ floating-point operations/s).

Most of the discrepancies between the nonlinear solutions and the TSFOIL data are primarily due to the relatively coarse grid used to compute the outer solutions. This was especially important at the higher Mach numbers at which shock waves extended into the outer region. However, there was little advantage in further refining the mesh of the nonlinear solver since the resolution of the solution was already limited by the spacing between measurements along the boundary.

For all three cases the linear solutions are quite accurate at the upstream and downstream boundaries of the nonlinear domain. This justifies using linear theory to establish the boundary conditions at those boundaries for the nonlinear calculations. When the simpler boundary condition $\partial\phi/\partial n = 0$ (exact for infinitely remote boundaries) was applied along the finite far-field boundaries of the nonlinear domain, the errors of the nonlinear solutions increased significantly. This is illustrated for the case $M = 0.90$ by the solid line in Fig. 2. The far-field boundaries clearly would have to be far more remote for this approximation to be appropriate.

Figure 2 gives only a first-order indication of how omission of nonlinear terms in the outer-flow solution would affect flow near the airfoil in an adaptive-wall test section. Enforcing the linear rather than the nonlinear outer-flow solution would suppress peak axial velocities above the airfoil, thus shifting the shock wave on the airfoil upstream of its free-air position. To quantify this effect, it would be necessary to compare the inner-flow solution (TSFOIL) that matches the linear outer-flow solution at the measurement level with the inner-flow solution that matches the nonlinear outer-flow solution. This is beyond the scope of this Note.

## Conclusions

For the cases considered here, nonlinear effects were important in the outer-flow solution when the outer flow included supersonic flow. Linear theory was adequate as long as the outer flow was everywhere subcritical. The important nonlinear effects could be approximated by solving the TSP equation on a very coarse grid. Furthermore, computation time was saved by confining the nonlinear calculation to a small domain and using linear theory to estimate nonzero free-air conditions along its far-field boundaries rather than applying $\partial\phi/\partial n = 0$ along more remote boundaries.

## References

[1]Sears, W. R., "Self-Correcting Wind Tunnels," *Aeronautical Journal,* Vol. 78, Feb.-March 1974, pp. 80–89.

[2]Binion, T. W., Jr., "Wall Interference in Wind Tunnels," AGARD CP 335, Sept. 1982.

[3]Ganzer, U., "A Review of Adaptive Wall Wind Tunnels," *Progress in Aerospace Science,* Vol. 22, No. 2, 1985, pp. 81–111.

[4]Lewis, M. L., "Aerofoil Testing in a Self-Streamlining Flexible Walled Wind Tunnel," NASA CR-4128, May 1988.

[5]Kraft, E. M., and Parker, R. L., Jr., "Experiments for the Reduction of Wind Tunnel Wall Interference by Adaptive-Wall Technology," Arnold Engineering Development Center, Arnold Air Force Station, TN, AEDC-TR-79-51, Oct. 1979.

[6]Erickson, J. C., Jr., Wittliff, C. E., Padova, C., and Homicz, G. F., "Adaptive-Wall Wind-Tunnel Investigations," Calspan, Buffalo, NY, Rept. RK-6040-A-2, Feb. 1981.

[7]Chen, A. W., Dickson, L. J., and Rubbert, P. E., "A Far-Field Matching Method for Transonic Computations," *AIAA Journal,* Vol. 15, No. 10, 1977, pp. 1491–1497.

[8]Lo, C. F., and Sickles, W. L., "A Hybrid Method of Transonic Computation with Application to the Adaptive Wind Tunnel," presented at the 8th U.S. National Congress of Applied Mechanics, Los Angeles, CA, June 26–30, 1978.

[9]Niederdrenk, P., and Wedemeyer, E., "Analytic Near-Field Boundary Conditions for Transonic Flow Computations," *AIAA Journal,* Vol. 25, No. 6, 1987, pp. 884–886.

[10]Lottati, I., "Implicit, Nonswitching, Vector-Oriented Algorithm for Steady Transonic Flow," *AIAA Journal,* Vol. 21, No. 11, 1983, pp. 1601–1603.

[11]Davis, S. S., "A Compatibility Assessment Method for Adaptive-Wall Wind Tunnels," *AIAA Journal,* Vol. 19, No. 9, 1981, pp. 1169–1173.

[12]Stahara, S. S., "Operational Manual for Two-Dimensional Transonic Code TSFOIL," NASA CR-3064, Dec. 1978.